Highly Sensitive Detection of DNA Hybridization on Commercialized Graphene-Coated Surface Plasmon Resonance Interfaces

ARTICLE *in* ANALYTICAL CHEMISTRY · OCTOBER 2014

Impact Factor: 5.64 · DOI: 10.1021/ac502705n · Source: PubMed

8 AUTHORS, INCLUDING:

Amaia Zurutuza
University of Strathclyde
29 PUBLICATIONS **932** CITATIONS

SEE PROFILE

Rabah Boukherroub
French National Centre for Scientific Research
448 PUBLICATIONS **7,387** CITATIONS

SEE PROFILE

analytical chemistry

Article

pubs.acs.org/ac

Highly Sensitive Detection of DNA Hybridization on Commercialized Graphene-Coated Surface Plasmon Resonance Interfaces

Oleksandr Zagorodko,[†] Jolanda Spadavecchia,[‡] Aritz Yanguas Serrano,[§] Iban Larroulet,[§] Amaia Pesquera,[∥] Amaia Zurutuza,[∥] Rabah Boukherroub,[†] and Sabine Szunerits*[,†]

[†]Institut de Recherche Interdisciplinaire, USR 3078 CNRS, Université Lille 1, Parc de la Haute Borne, 50 Avenue de Halley, BP 70478, 59658 Villeneuve d'Ascq, France

[‡]Laboratoire de Réactivité de Surfaces, UMR CNRS 7197, Université Pierre et Marie Curie—Paris VI, Site d'Ivry−Le Raphaël, 94200 Ivry-sur-Seine, France

[§]SENSIA SL, Poligono Aranguren, 9, Apartado de Correos 171, 20180 Oiartzun, Gipuzkoa, Spain

[∥]Graphenea S.A., Tolosa Hiribidea, 76, 20018 Donostia, San Sebastian, Spain

ABSTRACT: Strategies employed to interface biomolecules with nanomaterials have advanced considerably in recent years and found practical applications in many different research fields. The construction of nucleic acid modified interfaces together with the label-free detection of hybridization events has been one of the major research focuses in science and technology. In this paper, we demonstrate the high interest of graphene-on-metal surface plasmon resonance (SPR) interfaces for the detection of DNA hybridization events in the attomolar concentration range. The strategy consists on the noncovalent functionalization of graphene-coated SPR interfaces with gold nanostars carrying single-stranded DNA (ssDNA). Upon hybridization with its complementary DNA, desorption of the nanostructures takes place and thus enables the sensitive detection of the DNA hybridization event. The DNA sensor exhibits a detection limit of ≈500 aM for complementary DNA with a linear dynamic range up to 10^{-8} M. This label-free DNA detection platform should spur off new interest toward the use of commercially available graphene-coated SPR interfaces.

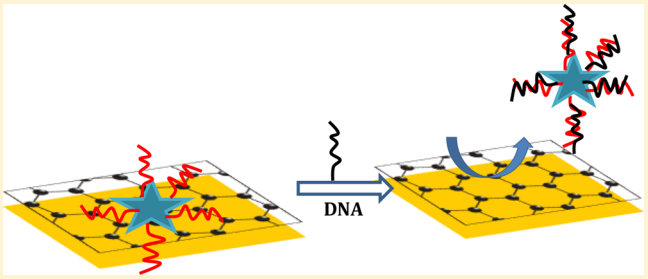

Surface plasmon resonance spectroscopy (SPR) has become a widely used and accepted bioanalytical technique for real-time detection and monitoring of biological binding events at a solid interface.[1] Since the commercialization in 1990 by Biacore (GE Healthcare), several SPR instruments with modified optical and liquid handling designs have been introduced to the market. While SPR has shown its potential as alternative to conventional biochemical methods for studying bimolecular interactions in a wider range of fields,[2] the nanomolar sensitivity achieved with conventional SPR instruments is insufficient for quantification of gene expression and for the detection of cancer markers, which ~~requires~~ femtomolar to attomolar level of nucleic acid detection.[3] Many different approaches have been explored to improve the sensitivity of SPR for DNA hybridization analysis. Fang et al. realized the detection of microRNAs down to 10 fM through a combination of surface poly(A) enzyme chemistry and nanoparticles amplified SPR measurements.[4] A femtomolar SPR detection of DNA−PNA hybridization with the assistance of DNA-guided polyaniline deposition has been developed by Su et al.[5] He et al. reported on a sandwich approach to detect DNA hybridization with a picomolar sensitivity.[6]

Lately, graphene oxide,[7] reduced graphene oxide (rGO),[7c,8] and graphene[9] have been investigated as coatings of SPR chips with the aim to increase the sensitivity of detection. The excellent optical properties and increased adsorption of biomolecules through hydrogen bonding and/or $\pi-\pi$-stacking interactions ~~makes~~ graphene and its derivatives good supporting layers for biomolecules' immobilization. One of the first applications on graphene-on-metal based SPR described in the literature relies on the capacity of α-thrombin to strip off a specific aptamer away from the rGO surface.[8a] Our group has shown that gold SPR chips modified with rGO through electrophoretic deposition approach can be used for lyzozyme sensing[8b] as well as for the investigation of bacteria binding affinities on the modified rGO surfaces.[10] Sensing of sugar−lectin interactions was recently explored on graphene[9c] and GO[7b] modified SPR interfaces. Nevertheless, graphene-on-metal SPR has until now hardly ever been used outside research centers, as graphene-coated gold chips were not commercially available. In a search for widening the access to graphene-based SPR, we developed a commercial SPR sensing platform with the ability to work with graphene-coated gold prisms. The transfer of single and few layered graphene sheets onto gold was achieved by chemical transfer of CVD grown graphene sheets.[9c,11] In this work, we show that these interfaces when integrated into the SENSIA SPR

Received: July 21, 2014
Accepted: October 23, 2014

   dx.doi.org/10.1021/ac502705n | *Anal. Chem.* XXXX, XXX, XXX−XXX

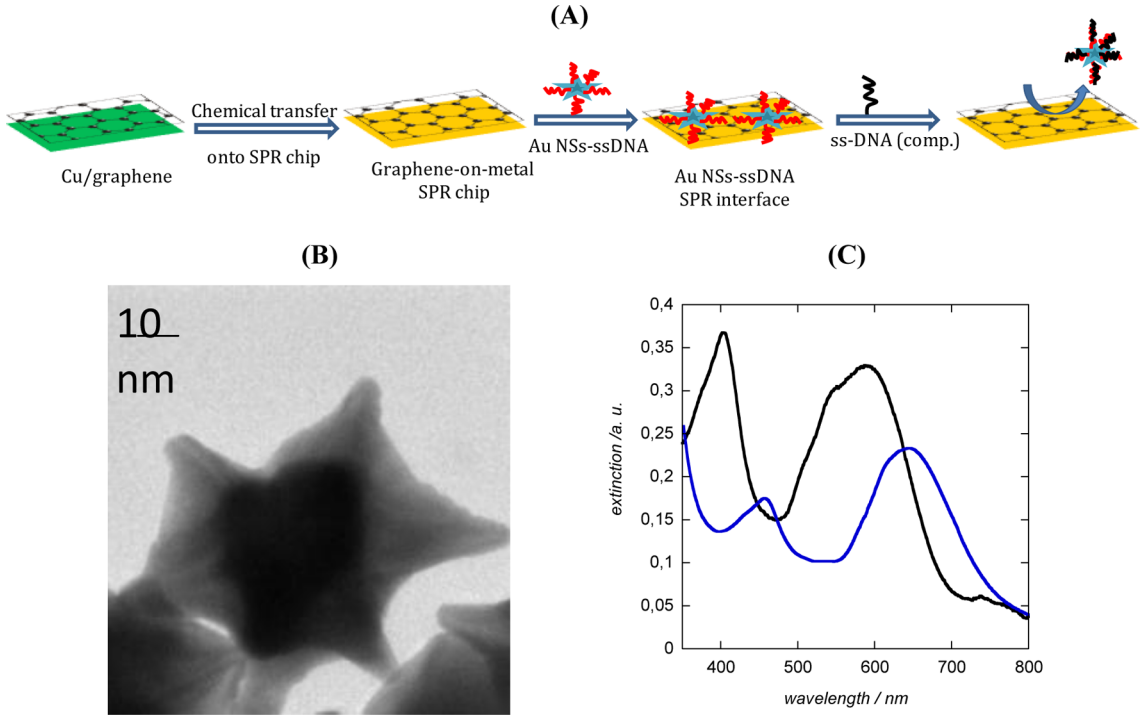

Figure 1. (A) Schematic illustration of the strategy employed to detect DNA hybridization events. (B) Typical TEM image of gold nanostars (Au NSs). (C) LSPR spectra of Au NSs (black) and DNA-modified Au NSs (blue) recorded in PBS aqueous solution.

instrument allow for attomolar level detection of nucleic acid hydridization in an easy and reproducible manner.

EXPERIMENTAL SECTION

Materials. All chemicals were reagent grade or higher and were used as received unless otherwise specified. Sodium hydroxide (NaOH), sodium chloride (NaCl), sodium dodecyl sulfate (SDS), salmon sperm DNA, formamide, phosphate buffer (PBS, 0.1 M, pH 7.4), acetone, acetonitrile (CH_3CN), methanol (CH_3OH), cetyltrimethylammonium bromide (CTAB), tetrachloroauric acid ($HAuCl_4$), silver nitrate ($AgNO_3$), sodium borohydride ($NaBH_4$), ascorbic acid, protoporphyrin IX (95%), ethylenediaminetetraacetic acid, and ethanol (C_2H_5OH) were purchased from Sigma-Aldrich. Saline sodium citrate buffer (SSC) was obtained from Fluka.

The oligonucleotides were purchased from Eurogentec and have the following sequences: DNA on gold nanostars, 5′-SH–$(T)_{15}$-AAG-CGA-TCG-ATA-GTC; complementary DNA, 3′-TTC-GCT-AGC-TAT-CAG-5′; noncomplementary DNA (three base mismatch, probe 3), 3′-TT**A**-GCT-AG**A**-TAT-CA**A**-5′.

Stock solutions of 5 μM were prepared in PBS buffer (100 mM, pH 7.4). The hybridization buffer was a solution of NaCl (0.5 M), phosphate buffer solution (0.01 M), and ethylenediaminetetraacetic acid (0.01 M, pH 5.5).

Gold Nanostars and DNA-Modified Gold Nanostars. *Formation of Gold Nanostars (Au NSs).* Gold nanostars were obtained when protoporphyrin IX was added in both the seed and the growth solutions, following the seed-mediated procedure.[12] Briefly, gold seeds were prepared by adding 5 mL of protoporphyrin IX (6.3×10^{-4} M) in EtOH/H_2O (3:2) to 5 mL of CTAB (0.20 M) at 27 °C under stirring conditions. After 5 min, 5 mL of an aqueous solution containing $HAuCl_4$ (2.5×10^{-4} M) was added for 10 min. To the resulting solution, 0.6 mL of ice-cooled $NaBH_4$ (0.01 M) was added dropwise followed by rapid stirring and kept without agitation for 4 h. The growth solution was prepared by adding 5 mL of CTAB (0.20 M) to 5 mL of protoporphyrin (6.29×10^{-4} M) and $AgNO_3$ (0.25 mL; 4×10^{-3} M) and stirring for 10 min. After this time, 5 mL of $HAuCl_4$ (1×10^{-3} M) was transferred to the mixture, and 70 μL of ascorbic acid (8×10^{-3} M) was added until decoloration of solution. Finally, after 4 h, 12 μL of seed solution was added to a growth solution and kept for 20 min without agitation. The obtained gold nanostars solution was centrifuged at 11 000 rpm for 26 min three times, and then the supernatant was discarded and the residue was redispersed in an equivalent amount of buffer solution (PBS, pH 7). This was repeated twice principally to remove the excess of CTAB. The final concentration of Au NSs was 5 μM.

Bioconjugation of Au NSs with ssDNA. Au NSs were chemically modified with ~~a~~ 5′-thiol-capped 30 base oligonucleotides according to the procedure described by Mirkin et al.[13] All oligonucleotides used in this study were synthesized on the basis of a previously characterized plant gene. In particular, our study is based on the *Agonum carbonarium* DNA sequences involved in the biosynthesis of ~~tricohothecenes~~ mycotoxins. To 200 μL of Au NSs solution (20 nM in 0.1 M PBS) was added 25 μL of 100 nM HS-DNA solution. After standing for 16 h, the solution was mixed with 0.25 mL of 10% NaCl. Next the Au NSs/HS-DNA was centrifuged twice at 6000 rpm for 20 s to remove HS-DNA in excess and particles were redispersed in PBS buffer (1 M NaCl, 100 mM phosphate buffer, pH 7). The resultant colloidal solution was sonicated for 5 min and then stirred for 1 h at room temperature.

Fabrication of Graphene-on-Metal SPR Interfaces. The graphene-on-metal SPR prisms were kindly provided by SENSIA. Gold-based SPR interfaces were formed by depositing 2 nm of titanium and 47 nm of gold successively onto cleaned glass made semicylindrical prims by sputtering under vacuum process.

dx.doi.org/10.1021/ac502705n | *Anal. Chem.* XXXX, XXX, XXX−XXX

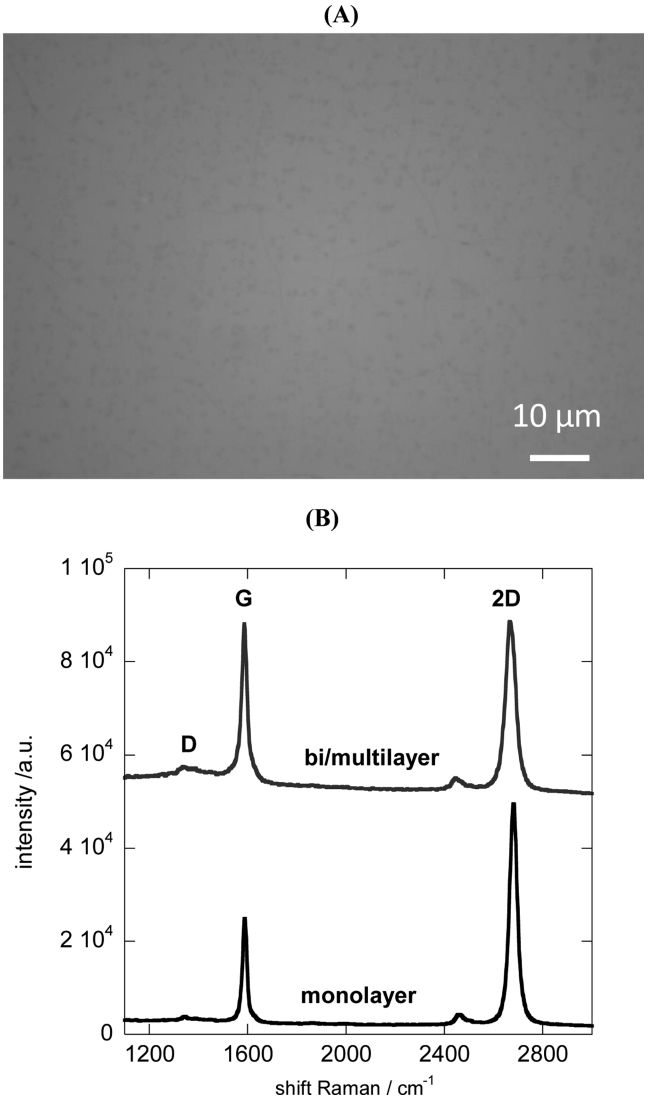

Figure 2. (A) SEM images and (B) Raman spectra of bright areas (monolayer) and darker areas (bi/multilayer) of the graphene-on-metal SPR interface.

Graphene was synthesized on polycrystalline Cu foils (25 μm thick Alfa-Aesar, purity 99.98%) in a cold-walled chemical vapor deposition (CVD) reactor as reported previously.[14] The Cu foils were annealed at 1000 °C under the flow of H_2 and Ar prior to graphene growth. Then, CH_4 was added to carry out the graphene growth. Finally, the sample was cooled under Ar atmosphere.

The CVD grown graphene was transferred onto gold SPR interfaces by a modified wet chemical transfer process as reported by Li et al.[14] Briefly, poly(methyl methacrylate) (PMMA, Microchem 495k) was spin-coated onto the graphene-coated Cu foil. The PMMA/graphene/Cu sample was baked at 150 °C for 2 min and then slowly cooled to room temperature. Backside graphene was removed by oxygen plasma treatment. Copper was dissolved using a commercial copper etchant solution (Transene). Graphene/PMMA was rinsed with deionized water 5−6 times to remove any ion contamination. Finally, the graphene was transferred onto the SPR substrate. After 10 min (for natural removal of water underneath the graphene), another slow backing step at 90 °C was carried out to remove the trapped water and to increase the contact between graphene and the substrate. Subsequently, the PMMA layer was removed by dipping the sample in acetone for 30 min. The SPR substrate with the transferred graphene was then rinsed with isopropyl alcohol and dried by mild nitrogen blow.

Modification of Graphene-on-Metal SPR Interfaces with Au NSs−ssDNA. The Au NSs−ssDNA solution (120 μL, 1 μM in PBS) was injected over the graphene-modified SPR interface at a flow rate of 7 μL min^{-1} and washed with PBS buffer at a flow rate of 10 μL min^{-1} for 10 min. Complementary and noncomplementary DNA (120 μL, 1 aM to 1 μM) in PBS were injected at a flow rate of 7 μL min^{-1}, and the hybridization signal was recorded. Regeneration of the graphene-on-metal interface between experiments was achieved by rinsing sequentially with urea (8 M), water, and PBS buffer. At the end of the experiment, the graphene-on-metal interface was further cleaned by immersing the interface into aqua regia (nitric acid/~~hydrochloric~~ acid = 1/3) for 1 min to remove any gold nanoparticles left on the graphene interface, followed by UV/ozone cleaning for 5 min (Jelight benchtop device, model 42-220, U.S.A.) to destroy organic matter.

Characterization. *Raman.* Micro-Raman spectroscopy measurements were performed on a Horiba Jobin Yvon LabRam HR micro-Raman system combined with a 473 nm (1 mW) laser diode as excitation source. Visible light is focused by a 100× objective. The scattered light is collected by the same objective in backscattering configuration, dispersed by a 1800 mm focal length monochromator and detected by a CCD camera.

Scanning Electron Microscopy (SEM). SEM images were obtained using an electron microscope ULTRA 55 (Zeiss) equipped with a thermal field emission emitter and a high-efficiency In-lens or ESB/SE detector. The SEM measurements were recorded at 3 kV for a better contrast between the substrate and the graphene overlayer.

SPR Instrumentation. SPR measurements were performed with a ~~commercial~~ available SPR instrumentation called "Indicator" provided by SENSIA (Spain) working at 650 nm. The instrument is equipped with a two-channel flow cell system which can be modeled as a 12 mm long cell with an inner diameter of 0.5 mm. The flow speed can be adjusted from 4 to 100 μL min^{-1}. Each of the loops has a volume of 60 μL. The prisms used have a refractive index of $n = 1.569$ (HBAK1, Schott) and have been modified by a Ti adhesion layer of 2 ± 0.5 nm and a gold thin film of 47 ± 2 nm deposited both by sputtering under vacuum.

RESULTS AND DISCUSSION

The strategy adopted for the ~~high-sensitivity~~ detection of DNA hybridization events on graphene-modified SPR chips is depicted in Figure 1A. The graphene-on-metal SPR interfaces used in this study were provided by SENSIA. High-quality and uniform graphene films on copper substrates were produced following a protocol developed by Li et al.[14] Transfer of the graphene sheets onto the gold SPR prism was achieved by a wet chemical transfer procedure according to Reina et al.[11] and lately reported by us.[9c] A typical SEM image of the graphene-on-metal SPR interfaces is exhibited in Figure 2A. The color contrast in the SEM image is correlated to the number of graphene layers transferred onto the SPR chip.[14] The thicker the graphene, the lower is the number of secondary electrons, so that multilayer (or bilayer) graphene appears darker than monolayers. Raman spectroscopy (Figure 2B) confirmed the presence of mono- and multilayer graphene on gold (Figure 2B). A defect peak at 1359 cm^{-1} is also seen, resulting from the wet chemical transfer process.

dx.doi.org/10.1021/ac502705n | Anal. Chem. XXXX, XXX, XXX−XXX

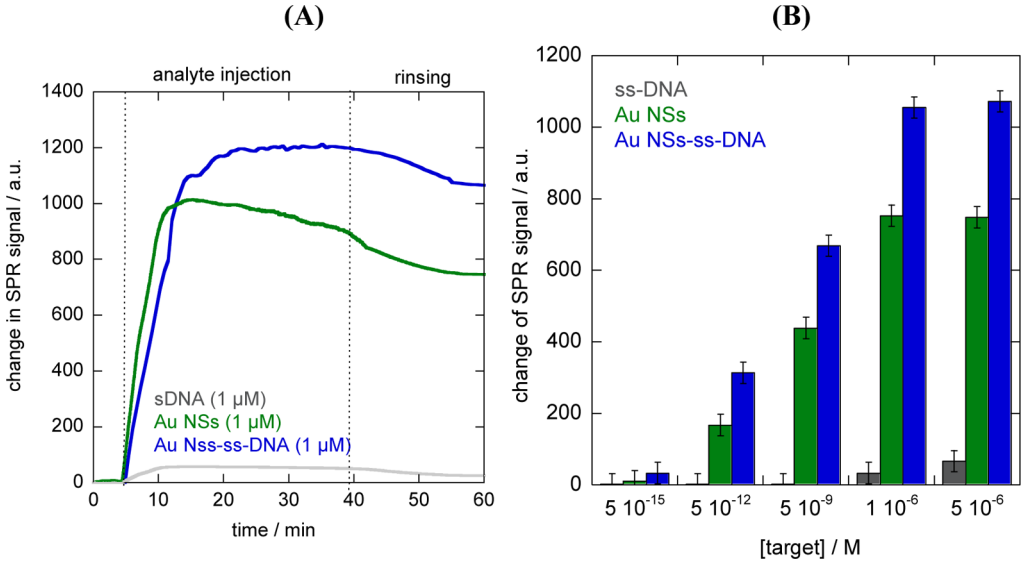

Figure 3. (A) Temporal change of SPR signal upon injection of ssDNA (1 μM, gray), Au NSs (1 μM, green), and Au NSs−ssDNA (1 μM, blue) onto graphene-modified SPR interfaces. (B) Bar diagram of SPR signal change depending on target (ssDNA, Au NSs, Au NSs−ssDNA) ~~and concentration~~ (5×10^{-15} to 5×10^{-6} M).

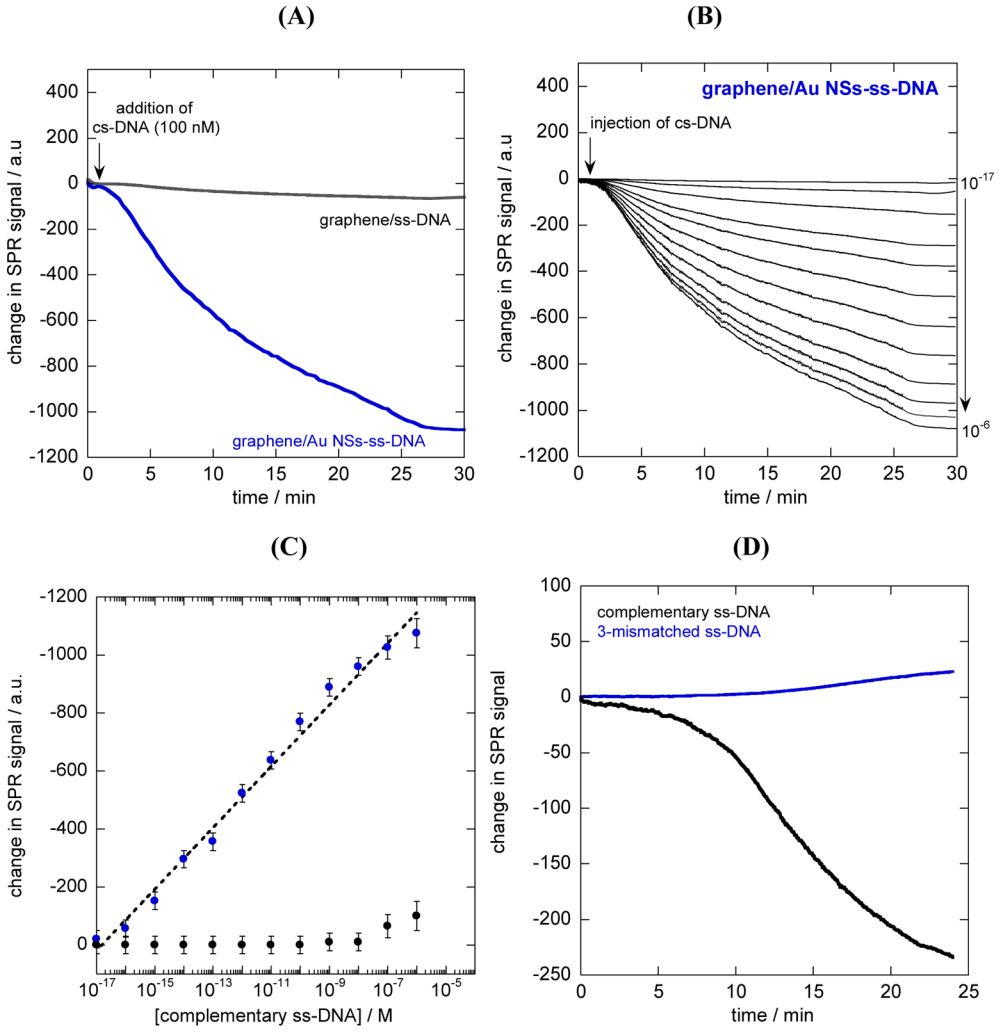

Figure 4. (A) Shift of SPR signal upon the addition of 100 nM complementary DNA (csDNA) onto ssDNA-modified graphene (gray) and Au NSs−ssDNA-modified graphene (blue). (B) Change in SPR signals upon addition of different csDNA concentrations (10^{-17} to 10^{-6} M). (C) Calibration curve for increased concentration of csDNA target on graphene/Au NS−ssDNA (blue) and graphene/ssDNA (black) (each response was measured in triplicate). (D) Discrimination between complementary (5 fM, black) and three-mismatched DNA (5 fM, blue) on Au NSs−ssDNA-modified graphene.

dx.doi.org/10.1021/ac502705n | *Anal. Chem.* XXXX, XXX, XXX−XXX

Table 1. Comparison of Sensitivities in DNA Analysis Using SPR and Other Analytical Techniques

detection method	LOD	ref
fluorescence	≈600 fM	19
SPR	150 nM	20
without amplification		
SPR	10 pM	6
gold nanoparticles amplification		
SPR	100 fM	5
with assistance of DNA-guided polyaniline deposition		
SPRi	10 fM	4
poly(A) and gold nanoparticles amplification		
SPR	10 fM	21
rGO and gold nanoparticles		
SPR	≈500 aM	this work
graphene and gold nanostars		
fiber-optic SPR	500 nM	22
colorimetric detection	≈10 nM	23
based on gold nanoparticles aggregation		
localized surface plasmon resonance (~~LSRP~~)	200 pM	12
LSPR	2 nM	24
amplification with doxorubicin-modified gold nanoparticles		
biobar code amplified scanometric method	500 aM	25
electrical	500 fM	26
Au nanoparticles and silver amplification		
chemiluminescence	5 fM	27
silver nanoparticles		

The amount of monolayer graphene transferred under our experimental conditions accounts to almost 95%.

The temporal change in the SPR signal upon injection of ssDNA (1 μM), Au NSs (1 μM), and Au NSs−ssDNA (1 μM) at a flow rate of 10 μL min^{-1} is depicted in Figure 3A. In the case of ssDNA, a noticeable change in the SPR signal can be detected due to the strong interaction of DNA and graphene.[15] The interaction of ssDNA toward graphene is indeed facilitated by partial deformation of the double helix of DNA due to the hydrophobic and/or π-stacking interactions of the DNA nucleobases with graphene. The SPR signal change could be significantly amplified using Au NSs and Au NSs chemically modified with a 5′-thiol-capped 30 base oligonucleotides ssDNA (Au NSs−ssDNA). After injection of the particles, PBS was flown over the interfaces. The SPR angle decreased gradually for the first minutes, before a steady-state value was reached. This suggests that some of the ~~Au Ns~~ and Au NSs−ssDNA structures desorb from the graphene surface ~~as the graphene surface~~ as they are either not in direct contact with graphene or too loosely bound. However, a stable SPR signal could be reached after 15 min ensuring the credibility of the following DNA hybridization experiments.

The fundamental idea behind SPR signal amplification is that the artificial increased mass of the analyte due to the linked Au NSs results in higher refractive index change on the SPR surface, leading to larger SPR shift.[16] This is, furthermore, amplified by the increased amount of analyte loaded onto the Au NSs. In addition, signal enhancement due to electromagnetic field coupling between the plasmonic properties of the nanostructures and propagating plasmons is expected. The CTAB-stabilized Au NSs display absorption bands at 402 nm due to interband transition,[17] and at 587 nm due to the rather short branches (Figure 1C). Au NSs modified with ssDNA show red-shifted plasmon bands at 457 and 643 nm, closely located near the 650 nm used in the SENSIA SPR instrument to excite propagating SPR waves. From the bare diagram in Figure 3B, the change in the SPR signal upon interaction of the three different targets (ssDNA, Au NSs, Au NSs−ssDNA) at different concentrations is displayed. As expected, the bare Au NSs show 20 times larger SPR changes than ssDNA alone. Moreover, Au NSs−ssDNA induce SPR signal amplification beyond that of Au NSs alone pointing toward a synergetic effect of ssDNA binding to graphene and signal amplification by Au NSs. An increase from 1 to 5 μM target did not alter the final SPR signal.

The ssDNA and Au NSs−ssDNA (1 μM) modified graphene−SPR interfaces were further investigated to detect hybridization events. The SPR responses upon addition of 100 nM complementary ssDNA are displayed in Figure 4A. In both cases, a decrease in the SPR signal is observed, being several times larger in the case of Au NSs−ssDNA-modified graphene SPR chip. As double-stranded DNA has a low affinity to graphene, hybridized targets are easily desorbed from the graphene interface, resulting in a negative shift of the SPR signal.[18] To determine the sensitivity and the detection limit of this approach, changes in SPR signals upon injection of different concentrations of complementary DNA were recorded (Figure 4B). Between each addition of DNA, the graphene-on-metal interface was regenerated with urea (8 M), water, and hybridization buffer at a flow of 10 μL min^{-1}. From the data recorded in Figure 4B, a calibration curve could be established (Figure 4C). The SPR signal changes linearly with the logarithm of the DNA concentration, rather in a linear manner, with a correlation coefficient of r = 0.994 according to ΔSPR = (−1782−106)(log[complementary sDNA]). In the case of Au NSs−ssDNA-modified graphene, the detection limit of complementary DNA was determined to be ≈500 aM from five black noise signals (95% confidence level), while on ssDNA-modified graphene only concentrations above 10 × 10^{-9} M show a change in SPR signal. This low detection limit, when compared to other DNA detection techniques and other plasmonic based

dx.doi.org/10.1021/ac502705n | Anal. Chem. XXXX, XXX, XXX−XXX

methods (Table 1), is believed to be a consequence of the SPR signal amplification using the Au NSs, its plasmonic coupling effect, and the efficient adsorption of the nanostructures to the graphene matrix. The sensor interface shows in addition good discrimination to mismatched samples. A three-mismatched DNA sample results in an increase rather than a decrease in SPR signal, due to its accumulation on the surface rather than from its desorption. It is thus a very direct manner to screen for complementary DNA strands.

CONCLUSION

In conclusion, we have used commercially available graphene-coated SPR interfaces to study their loading capacity with gold nanostars, ssDNA, and gold nanostars functionalized with DNA strands and their subsequent use to study DNA hybridization events. SPR signal amplification was observed using Au NSs and Au NSs modified with ssDNA. The Au NSs interacted strongly with graphene and enabled in an easy manner the integration of ssDNA onto graphene nanosheets. Interaction with complementary DNA sequence resulted in the formation of double-stranded DNA and desorption of the nanostructures from the graphene matrix. The DNA sensor exhibits a detection limit of ≈500 aM for complementary DNA with a linear dynamic range up to 10^{-8} M. Discrimination between mismatched DNA is achieved. This label-free DNA detection platform should spur off new interest toward the use of commercially available graphene-coated SPR interfaces. As the presented work concerned the development of a new analytical concept for the study of gene expression and cancer biomarker, buffer samples spiked with known concentrations of target analytes were used. The analysis of real samples such as blood plasma should be possible with this approach but might need some optimization to be carried out.

AUTHOR INFORMATION

Corresponding Author

*E-mail: sabine.szunerits@iri.univ-lille1.fr.

Notes

The authors declare no competing financial interest.

ACKNOWLEDGMENTS

R.B. and S.S. gratefully acknowledge financial support from the Centre National de la Recherche Scientifique (CNRS), the University Lille 1, and the Nord Pas de Calais region. S.S. thanks the Institut Universitaire de France (IUF) for financial support.

REFERENCES

(1) (a) Homola, J.; Yee, S. S.; Gauglitz, G. *Sens. Actuators, B* **1999**, *54*, 3. (b) Hoa, X. D.; Kirk, A. G.; Tabrizian, M. *Biosens. Bioelectron.* **2007**, *23*, 151. (c) Scarano, S.; Mascini, M.; Turner, A. P. F.; Minunni, M. *Biosens. Bioelectron.* **2010**, *25*, 957.

(2) Homola, J. *Chem. Rev.* **2008**, *108*, 462.

(3) Wang, J. *Small* **2005**, *1*, 1036.

(4) Fang, S.; Lee, H. J.; Wark, A. W.; Corn, R. M. *J. Am. Chem. Soc.* **2006**, *128*, 14044.

(5) Su, X.; Teh, H.; Aung, K. M. M.; Zong, Y.; Gao, Z. *Biosens. Bioelectron.* **2008**, *23*, 1715.

(6) He, L.; Musick, M. D.; Nicewarner, S. R.; Salinas, F. G.; Benkovic, S. J.; Natan, M. J.; Keating, C. D. *J. Am. Chem. Soc.* **2000**, *122*, 9071.

(7) (a) Xue, T.; Cui, X.; Chen, J.; Liu, C.; Wang, Q.; Wang, H.; Zhen, W. *ACS Appl. Mater. Interfaces* **2013**, *5*, 2096. (b) Huang, C.-F.; Yao, G.-H.; Liang, R.-P.; Qiu, J.-D. *Biosen. Bioelectron.* **2013**, *50*, 305. (c) Xue, T.; Cui, X.; Gu[illegible]W.; Wang, Q.; Liu, C.; Wang, H.; Qi, K.; Singh, D. J.; Zheng, W. *Biosen. Bioelectron.* **2014**, *58*, 374.

(8) (a) Wang, L.; Zhu, C.; Han, L.; Jin, L.; Zhou, M.; Dong, S. *Chem. Commun.* **2011**, *47*, 7794. (b) Subramanian, P.; Lesniewski, A.; Kaminska, I.; Vlandas, A.; Vasilescu, A.; Niedziolka-Jonsson, J.; Pichonat, E.; Happy, H.; Boukherroub, R.; Szunerits, S. *Biosens. Bioelectron.* **2013**, *50*, 239.

(9) (a) Wu, L.; Chu, H. S.; Koh, W. S.; Li, E. P. *Opt. Express* **2010**, *18*, 14395. (b) Salihoglu, O.; Balci, O.; Kocabas, C. *Appl. Phys. Lett.* **2011**, *100*, 213110. (c) Penezic, A.; Deokar, G.; Vinaud, D.; Pichonat, E.; Subramanian, P.; Gašparovi, B.; Boukherroub, R.; Szunerits, S. *Plamonics* **2014**, *9*, 677.

(10) Subramanian, P.; Bar[illegible]buaifel, F.; Bouckaert, J.; Yamakawa, N.; Boukerroub, R.; Szunerits, S. *ACS Appl. Mater. Interfaces* **2014**, ~~in press.~~

(11) Reina, A.; Son, H.; Jiao, L.; Fan, B.; Dresselhause, M. S.; Liu, Z. F.; Kong, J. *J. Phys. Chem. C* **2008**, *122*, 17741.

(12) Spadavecchia, J.; Barras, A.; Lyskawa, J.; Woisel, P.; Laure, W.; Pradier, C.-M.; Boukherroub, R.; Szunerits, S. *Anal. Chem.* **2013**, *85*, 3288.

(13) Mirkin, C. A.; Letsinger, L. R.; Mucic, C. R.; Storhof, J. J. *Nature* **1996**, *382*, 607.

(14) Li, W.; Cai, W.; An, J.; Kim, S.; Nah, J.; Yang, D.; Piner, R.; Velamakanni, A.; Jung, I.; Tutuc, E.; Banerjee, S. K.; Colombo, L.; Ruoff, R. S. *Science* **2009**, *324*, 1312.

(15) (a) Tang, L. A. L.; Wang, J.; Loh, K. P. *J. Am. Chem. Soc.* **2010**, *132*, 10976. (b) Varghese, N.; Mogera, U.; Govindaraj, A.; Das, A.; Maiti, P. K.; Sood, A. K.; Rao, C. N. R. *ChemPhysChem* **2009**, *10*, 206. (c) Tang, Z.; Wu, H.; Cort, J. R.; Buchko, G. W.; Zhang, Y.; Shao, Y.; Aksay, I. A.; Liu, J.; Lin, Y. *Small* **2010**, *6*, 1205. (d) Akca, S.; Foroughi, A.; Frochtzwajg, D.; Postman, H. W. C. *PLoS One* **2011**, *6*, e18442. (e) Manna, A. K.; Pati, S. K. *J. Mater. Chem. B* **2013**, *1*, 91.

(16) (a) Hutter, E.; Cha, S.; Liu, J.-F.; Park, J. W.; Yi, J.; Fendler, J. H.; Roy, D. *J. Phys. Chem. B* **2001**, *105*, 8. (b) Lyon, L. A.; Musick, M. D.; Natan, M. J. *Anal. Chem.* **1998**, *70*, 5177. (c) He, L.; Musick, M. D.; Nicewarner, S. R.; Salinas, F. G.; Benkovic, S. J.; Natan, M. J.; Keating, C. D. *J. Am. Chem. Soc.* **2000**, *122*, 9071. (d) Matsui, J.; Akamastu, K.; Hara, N.; Miyoshi, D.; Nawafune, H.; Tamaki, K.; Sugimoto, N. *Anal. Chem.* **2005**, *77*, 4282. (e) Li, Y.; Wark, A. W.; Lee, H. J.; Corn, R. M. *Anal. Chem.* **2006**, *78*, 3158.

(17) (a) Zach, M.; Kasemo, B.; Langhammer, C. *ACS Nano* **2011**, *5*, 2535. (b) Dulkeith, E.; Niedereichholz, T.; Klar, T. A.; Feldmann, J.; von Plessen, G.; Gittins, D. I.; Mayya, K. S.; Caruso, F. *Phys. Rev. B* **2004**, *70*, 205424. (c) Beversluis, M. R.; Bouhelier, A.; Novotny, L. *Phys. Rev. B* **2003**, *68*, 115433.

(18) Wu, M.; Kempaiah, R.; Huang, P.-J. J.; Maheshwari, V.; Loiu, J. *Langmuir* **2011**, *27*, 2713.

(19) Rosi, N. L.; Mirkin, C. A. *Chem. Rev.* **2005**, *105*, 1547.

(20) Kai, E.; Sawata, S.; Ikebukuro, K.; Ida, T.; Honda, T.; Karube, I. *Anal. Chem.* **1999**, *71*, 796.

(21) Xue, T.; Cui, X.-S.; Guan, W.; Wang, Q.; Liu, C.; Wang, H.-K.; Qi, K.; Singh, D. J.; Zhang, W. *Biosens. Bioelectron.* **2014**, *58*, 374.

(22) Pollet, J.; Delport, F.; Janssen, K. P. F.; Jans, K.; Maes, G.; Pfeiffer, H.; Wevers, M.; Lammertyn, J. *Biosens. Bioelectron.* **2009**, *25*, 864.

(23) Elghnian, R.; Storhoff, J. J.; Mucic, R. C.; Letsnger, R. L.; Mirkin, C. A. *Science* **1997**, *277*, 1078.

(24) Spadavecchia, J.; Perumal, R.; Barras, A.; Lyskawa, J.; Woisel, P.; Laure, W.; Pradier, C.-M.; Boukherroub, R.; Szunerits, S. *Analyst* **2014**, *139*, 157.

(25) Nam, J. M.; Stoeva, S. I.; Mirkin, C. A. *J. Am. Chem. Soc.* **2004**, *126*, 5932.

(26) Park, S.-J.; Taton, T. A.; Mirkin, C. A. *Science* **2002**, *295*, 1503.

(27) Liu, C.-H.; Li, Z.-P.; Du, B.-A.; Duan, X.-R.; Wang, Y.-C. *Anal. Chem.* **2006**, *78*, 3738.